


Article

Impact of Air Mass Conditions and Aerosol Properties on Ice Nucleating Particle Concentrations at the High Altitude Research Station Jungfraujoch

Larissa Lacher ^{1,*},[†], Martin Steinbacher ², Nicolas Bukowiecki ³, Erik Herrmann ³, Assaf Zipori ^{4,‡} and Zamin A. Kanji ^{1,*} 

¹ Institute for Atmospheric and Climate Science, ETHZ, 8092 Zurich, Switzerland

² Empa, Swiss Federal Laboratories for Materials Science and Technology, 8600 Duebendorf, Switzerland; martin.steinbacher@empa.ch

³ Laboratory of Atmospheric Chemistry, Paul Scherrer Institute, 5232 Villigen, Switzerland; nicolas.bukowiecki@psi.ch (N.B.); tmi.erik.herrmann@gmail.com (E.H.)

⁴ Institute for Earth Science, Hebrew University, Jerusalem 76100, Israel; assaf.zipori@mail.huji.ac.il

* Correspondence: larissa.lacher@kit.edu (L.L.); zamin.kanji@env.ethz.ch (Z.A.K.)

† Current address: Institute for Meteorology and Climate Research—Atmospheric Aerosol Research, KIT, 76021 Karlsruhe, Germany.

‡ Current address: Department of Earth and Planetary Sciences, Weizmann Institute of Science, Rehovot 7610001, Israel.

Received: 29 June 2018; Accepted: 1 September 2018; Published: 19 September 2018



Abstract: Ice nucleation is the source of primary ice crystals in mixed-phase clouds. Only a small fraction of aerosols called ice nucleating particles (INPs) catalyze ice formation, with their nature and origin remaining unclear. In this study, we investigate potential predictor parameters of meteorological conditions and aerosol properties for INP concentrations at mixed-phase cloud condition at 242 K. Measurements were conducted at the High Altitude Research Station Jungfraujoch (Switzerland, 3580 m a.s.l.), which is located predominantly in the free troposphere (FT) but can occasionally receive injections from the boundary layer (BLI). Measurements are taken during a long-term study of eight field campaigns, allowing for the first time an interannual (2014–2017) and seasonal (spring, summer, and winter) distinction of high-time-resolution INP measurements. We investigate ranked correlation coefficients between INP concentrations and meteorological parameters and aerosol properties. While a commonly used parameterization lacks in predicting the observed INP concentrations, the best INP predictor is the total available surface area of the aerosol particles, with no obvious seasonal trend in the relationship. Nevertheless, the predicting capability is less pronounced in the FT, which might be caused by ageing effects. Furthermore, there is some evidence of anthropogenic influence on INP concentrations during BLI. Our study contributes to an improved understanding of ice nucleation in the free troposphere, however, it also underlines that a knowledge gap of ice nucleation in such an environment exists.

Keywords: ice nucleation; free troposphere; INP parameterization

1. Introduction

The first formation of ice in clouds remains one of the most challenging processes to understand and to quantify in ice cloud formation. At temperatures warmer than and supersaturations lower than required for homogeneous nucleation [1], the crystallization of supercooled cloud droplets can only be initiated by aerosol particles termed ice nucleating particles (INPs) [2]. This heterogeneous pathway for ice crystal formation determines the existence of mixed-phase clouds (MPC), where both

liquid cloud droplets and ice crystals co-exist. Ice nucleation contributes to the number concentrations of ice crystals in MPCs. This parameter is key to the radiative properties, lifetime, and precipitation formation of such clouds, and which are a challenge to represent in models [3]. While secondary ice production is efficient down to temperatures of ~ 258 K [4], INPs remain the only source of primary ice formation currently known for colder MPC temperatures.

INPs are a rare subset of ambient aerosol particles and to date it is uncertain which type(s) of aerosol particles are dominating the ambient INP population in different atmospheric environments, and in different temperature regimes in the atmosphere [5]. In addition, the specific features of these particles triggering the phase change are not fully understood. A common concept is that INPs carry so-called ice-active sites [6] (e.g., such as steps, cracks, or hydrophilic locations on the INP surface), which stabilizes the forming ice embryo [6]. Being a surface specific feature, the probability of the occurrence of ice-active sites was found to scale with the total available surface area (A_{tot}) of the aerosols [7–9]. An aerosol particle type which was found to nucleate ice efficiently at temperatures $T < 253$ K is mineral dust (as summarized in e.g., [5,10]), which refers to particles being emitted from deserts and agricultural soils, which can contain organic and biogenic compounds, as well as volcanic mineral (ash) particles. Aerosols generated from living species, such as bacteria, fungi, lichens, pollen, and phytoplankton exudates, as summarized in [11], were also found to contribute to ambient INPs [12–17]. Other potential sources for INPs are emissions from biomass or fossil fuel burning [18–24], but the ability of combustion particles to nucleate ice is uncertain since contradicting results were found [25]. In the free troposphere (FT), an environment which is decoupled from direct emissions from boundary layer processes [26] and therefore rather well-mixed, different aerosol types might contribute to the INP population.

To date, several approaches exist to parameterize INP concentrations in global climate models. A first approach to predict INP concentrations is based on observed relationships between INP and temperature [27] or supersaturation [28], at which the INP measurements were performed. In these simple schemes, aerosol particles (size, chemistry, classes) are not explicitly modeled. However, in many field studies, it was found that the variability of INP concentrations for a given temperature and relative humidity (RH) can span several orders of magnitude [15,29–33], which provides evidence that single-predictor parameterizations are not capable of prescribing INP concentrations accurately. In fact, they ignore that heterogeneous formation of ice crystals depends on the available aerosol particle population and that the ice nucleation ability of single classes of aerosols is quite distinct. To improve on this, DeMott, et al. [15] related immersion freezing INP concentrations not only to the measurement temperature but also to the aerosol particle concentration >0.5 μm in diameter ($N_{>0.5 \mu\text{m}}$), which is based on field measurements from very different locations. It is also indicated that aerosol particles of smaller sizes might have a contribution to ice nucleation in the atmosphere [32, 34–40] and that the INP population is not only dominated by $N_{>0.5 \mu\text{m}}$. Another way to calculate INP concentrations is to simulate the spatial and temporal distribution of aerosol particles and define which particles are ice active [41–45]. The method is, however, limited by the possibility of yet unidentified ambient INPs and of processes influencing the ice nucleation. The parameterizations used in these simulations are usually based on laboratory studies on the ice activity of a certain class of aerosol particle. E.g., Niemand, et al. [46] uses laboratory studies on natural desert dust samples, activating in the temperature range 261–237 K in the immersion freezing regime. The parameterization proposed by Phillips, et al. [47] also incorporates black carbon (BC) as an INP. The latter is, however, in contrast to the results of two studies on the ice residuals in MPCs at the High Altitude Research Station Jungfraujoch (JFJ) during winter (MPC temperatures >247 K) by Kamphus, et al. [48] and Kupiszewski, et al. [49], where no major contribution of BC was found. This question the importance of BC to ice nucleation in MPCs [50,51]. To further improve parameterizations of INPs, field, laboratory, and modeling studies are needed to identify sources of INPs. As a first approach to do so, relationships between INPs and different parameters can be evaluated. In this study, we investigate the relationships of INP concentrations measured in the FT with meteorological variables, aerosol, and air mass properties.

We aim to improve our understanding of the control mechanisms for ice nucleation in the FT, which is of special interest since it is directly relevant for the formation of MPCs.

Meteorology might have an influence on INP as it was found by Lugauer, et al. [52] and Collaud Coen, et al. [53] that the aerosol transport to the High Altitude Research Station Jungfraujoch (JFJ) is influenced by atmospheric transport patterns. In turn, these patterns result in differences in the parameters of pressure and ambient RH (RH_a), which can thus be used as an indication for the underlying weather. In addition, RH_a gives an indication for the process of water uptake of the aerosols below water-saturated conditions, which might change the ice nucleation ability of the aerosol particles due to re-distribution or washing-off of ice-active sites, as was indicated in a study by Harrison, et al. [54], showing that the ice nucleation efficiency of some feldspar mineral dust particle decreased with time suspended in water. Next to RH_a , the contact with water of the INPs prior to sampling can be indicated by the presence of clouds at the sampling site. A differentiation between cloudy conditions and RH_a is thereby needed since INPs might be removed by precipitating clouds [55]. A first indication for the origin of the sampled air masses and thus INPs can be given by analysis of the wind direction. The reason to explore correlations with wind speed is related to blowing surface snow where ice crystals from the ground are advected into the sampling volumes. Since blowing snow is dependent on wind speed [56], clarification if this process, which might impact the INP sampling, is necessary.

Previous studies investigated the relationship of immersion mode INP concentrations with meteorological variables and the physical properties of aerosol particles. At the JFJ, Conen, et al. [57] found a correlation of INP concentrations measured at $T = 265$ K with air temperature (T_a), observing considerably lower INP concentrations at colder T_a . They attribute this finding to the activation and subsequent loss of INP in air masses prior to the arrival at the JFJ. In addition, only a weak correlation with $N_{>0.5 \mu\text{m}}$ was found, and no influence of SDEs on INP concentrations at this measurement temperature was indicated. Boose, et al. [30] measured INP concentrations in the immersion mode at $T = 241$ K in winter 2014 and found no relationship with T_a . This was explained by the measurement temperature being colder than T_a , which could mask a depletion of INP active at 241 K. No other relationship to the meteorological conditions was found in this study, but a moderate correlation of INP concentrations with $N_{>0.5 \mu\text{m}}$. At a similar measurement temperature of $T = 243$ K, but at a marine boundary layer site, Mason, et al. [16] also found a good correlation of INPs and $N_{>0.5 \mu\text{m}}$. Concerning the initial size of INPs, Mason, et al. [32] measured INPs at different ground level environments and revealed a strong contribution of coarse-mode particles to the INP population in general, but with a weaker contribution towards colder measurement temperatures [32]. In addition, size-dependent removal processes during the transport to elevated levels in the atmosphere might lead to a shift of the INP size distribution towards smaller sizes.

In order to improve our understanding on the control mechanism of INP concentrations on a time scale longer than that of an individual field study, we present an analysis of INP concentrations and ambient conditions based on a long-term study [58]. We investigate if there are seasonal trends in the correlation between INP concentrations and possibly predictor parameters under different sampling conditions with regard to FT sampling conditions, and also influences from boundary layer injections (BLI).

2. Material and Methods

2.1. Sampling Location and Conditions

Measurements were conducted at the High Altitude Research Station Jungfraujoch (JFJ), located in the Swiss Alps (3580 m a.s.l.; 46°33' N, 7°59' E). The site is located on a ridge between Mount Jungfrau and Mount Mönch and is surrounded by firn ice throughout the year. Due to its altitude, the site is situated in the lower FT but can be influenced by BLI. The latter is most prominent in the warm season and results in a seasonal cycle of aerosol particle concentration and population [52,53,59–61]. In addition, the station is regularly affected by Saharan dust events (SDE) [62] and air masses originating in the marine boundary layer [63], both of which are transported to the JFJ in the FT,

and can lead to elevated INP concentrations [30,58,64]. The JFJ is part of the Global Atmospheric Watch (GAW) monitoring project as well as of the ACTRIS2 Infrastructure (European Research Infrastructure for the observation of Aerosol, Clouds, and Trace gases), the Swiss National Air Pollution Monitoring Network (NABEL), and the Swiss meteorological network (SwissMetNet). As such, aerosol physical properties (total number concentration and size distribution of aerosol particles, their light absorption, scattering and backscattering coefficients, and the equivalent BC mass concentrations (eBC) are measured continuously e.g., [65,66]. Additionally, trace gases (carbon monoxide, carbon dioxide, nitrogen oxide, nitrogen dioxide, nitrous oxide, the sum of nitrogen oxides (NO_y), peroxyacetyl nitrate, sulfur dioxide, methane, and ozone; [67]) are continuously monitored, accompanied by measurements of meteorological conditions (T_a , RH_a , pressure, wind direction, wind velocity, and short- and longwave radiation [68]).

Trace gases and aerosol measurements are used here to discriminate FT conditions and episodes under influence of BLI (see Section 2.3). We categorize the sampled air masses into all conditions (sum of performed measurements), BLI, and background FT conditions ($FT_{background}$; in addition to BLI also excluding SDEs and marine air mass influence).

2.2. Experimental

The measurements were conducted during a total of 8 field campaigns in the years 2014–2017, out of which two were in spring (May/June), two in summer (July/August), and three in winter (January/February/March). Each field campaign represents 2 to 5 weeks sampling time (see Lacher, et al. [58] for a detailed description).

2.2.1. INP Concentrations

Ice nucleation measurements were conducted with the Horizontal Ice Nucleation Chamber (HINC [69]). HINC is a continuous flow diffusion chamber which measures INP concentrations with a time resolution of 20 min. The discussed INP concentrations in this work refer to measurements conducted at $T = 242 \pm 0.4$ K and in the immersion freezing mode (RH_w (RH with respect to water) = $104 \pm 1.5\%$), representing conditions relevant for MPC formation. The residence time of aerosol particles in the chamber was 8 s.

INP measurements were performed at the GAW inlet [70], and are representative for aerosol particles $<40 \mu\text{m}$ at wind speeds $<20 \text{ms}^{-1}$. The aerosol particle transmission efficiency in the inlet system and HINC is 74% for particles $<1 \mu\text{m}$ (56% for particles $<2 \mu\text{m}$; see Lacher, et al. [69] for more detail). Since particle concentrations $>1 \mu\text{m}$ are very rare for this site, the INP measurements are representative for the characteristic aerosol particle population at the JFJ [65,71].

2.2.2. Meteorological Parameters

In this study, the relationships of INP concentrations to the meteorological parameters of T_a , RH_a , pressure, wind velocity, and wind direction are explored. The meteorological measurements were taken by the Federal Office for Meteorology and Climatology MeteoSwiss and comply with the standards of the World Meteorological Organization. In- and out-of-cloud conditions were thereby inferred by the difference between T_a and the sky temperature, as described by Herrmann, et al. [60]. The sky temperature is calculated with the Stefan Boltzmann law, using the longwave irradiance measurements at the site. In the presence of a cloud, the longwave irradiance is received from the cloud, and the calculated sky temperature gives the temperature of the cloud and is similar to the ambient temperature. As such, small differences between the ambient and sky temperatures (~ 5 K) are used for determining in-cloud conditions.

2.2.3. Size Inferred Parameters

We investigate dependences of INP concentrations on aerosol concentrations (N) in specific size ranges, as inferred from the size distribution measurements. These measurements were obtained

from the GAW Scanning Mobility Particle Sizer (SMPS), consisting of a Differential Mobility Analyzer (DMA; 3071, TSI INCORPORATED, Shoreview, MN, USA) and a Condensation Particle Counter (CPC; 3775, TSI INCORPORATED, Shoreview, MN, USA), measuring in the size range 20–600 nm. The larger fraction of the size distribution is measured with an OPC (GRIMM Dust Monitor 1.108, GRIMM Aerosol Technique, Ainring, Austria) giving information on the particles' size in the range 0.23–16.4 μm . These measurements were also performed at the GAW inlet. The SMPS and OPC size distribution are merged by converting mobility and optical diameters to volume equivalent diameters, assuming a particle density of 1565 kg m^{-3} [71] and a unity shape factor. Based on the size distribution measurements of the aerosol particle population, A_{tot} is determined assuming spherical geometry.

The relationship of INP concentrations and N in three different size ranges are investigated, which represent the Aitken mode $<0.1 \mu\text{m}$ ($N_{<0.1 \mu\text{m}}$), the smaller fraction of accumulation mode particles between $0.1 \mu\text{m}$ and $0.5 \mu\text{m}$ ($N_{0.1-0.5 \mu\text{m}}$), and the larger fraction of the accumulation and coarse mode particles $>0.5 \mu\text{m}$ ($N_{>0.5 \mu\text{m}}$). In the field campaign of spring 2016, aerosol size distributions $>0.5 \mu\text{m}$ were not available due to a malfunction of the instrument.

2.2.4. Absorption and Scattering Measurements

To investigate the possible contribution of BC on ice nucleation, INP concentrations are evaluated against eBC . The eBC was measured with an aethalometer (AE31, MAGEE scientific, Berkeley, CA, USA) at the GAW inlet and was derived from the attenuation measurements by applying the factory standard mass attenuation cross sect. of $16.6 \text{ m}^2 \text{ g}^{-1}$ at 880 nm.

The single scattering albedo Angström exponent can be used to assess the influence from mineral dust at the JFJ. It is derived for wavelengths of 450 nm, 550 nm, and 700 nm from measurements of the total aerosol scattering coefficients (at three wavelengths) and the absorption coefficients (at seven wavelengths), which are measured by an integrating nephelometer (3563, TSI INCORPORATED, Shoreview, MN, USA) and the aethalometer, respectively.

2.2.5. Chemical Components

The analysis of chemical components is based on measurements of a known air volume via a quartz fiber filter (Pallflex XP56 Tissuquartz 2500QAT-UP, Pall Corporation, Port Washington, NY, USA) with a high-volume instrument (DA-80H, Digitel, Hegnau, Switzerland; [72]) of particulate matter (PM) below $10 \mu\text{m}$ (PM10) over 24 h. The species of interest are thereby sulfate and nitrate, which are secondary particles from sulfur dioxide and nitrogen oxides, respectively, and are mainly emitted from anthropogenic sources. As such, they can be used as a tracer for the same. In addition, sulfate can also be of marine origin, however, the better indication for marine-influenced air masses is chloride being emitted into the atmosphere as sodium chloride from oceans. Sulfate, nitrate, and chloride are extracted with pure water from the filter by agitation, and are determined by ion chromatography (Dionex, DX500, ThermoFisher, Waltham, MA, USA) eluent $8.0 \text{ mM Na}_2\text{CO}_3/1.0 \text{ mM NaHCO}_3$. PM10 filters are weighted before and after exposure to retrieve PM10 concentrations. More details on the standard analysis procedure can be found elsewhere [73].

2.2.6. Trace Gases

Trace gases are continuously measured at the JFJ as part of the GAW monitoring program, and are used in this study to determine FT conditions. The species of interest thereby are carbon monoxide (CO) and NO_y (total reactive nitrogen). CO is measured with a cavity ringdown spectrometer (G2401 [74], Picarro Inc., Santa Clara, CA, USA), and NO_y is measured with a highly sensitive nitrogen monoxide (NO) analyzer, based on chemiluminescence detection (CLD89p, Eco Physics, Duernten, Switzerland) after conversion of NO_y to NO on a heated gold catalyst.

2.2.7. Cloud Water Samples

Samples of cloud water were taken in parallel to the INP measurements [30,69]. The time resolution of these measurements are thereby determined by the liquid cloud water content. The cloud water samples are analyzed with an inductively coupled plasma mass spectrometer (ICP-MS, 7500cx, Agilent, Santa Clara, CA, USA,) as discussed in Zipori et al. [75,76].

2.2.8. Overview INP Predictor Parameters

All parameters which are tested against INP concentrations are listed in Table 1. The sampling time of the INP concentrations (20 min) is the common denominator for the averaging time of parameters that have a higher time resolution; parameters with a lower time resolution (RH_a and eBC) are interpolated between timestamps to match the INP timestamp. The low-time resolution of PM10 filters restricted the comparison to INP concentrations, since the latter were not measured continuously. As such, we only considered INP measurements which covered >9 h of the respective PM10 sampling interval.

Since in aerosol science many relationships are not linear in their nature, we investigate possible dependences between INP concentrations and the respective parameters with the Spearman's rank correlation coefficient [26]. This test is based on the relative rank of the data within the total sample and therefore investigates monotonic, but not necessarily linear relationships, and is less sensitive to outliers. We thereby consider relationships which are significant and those with correlation coefficients >0.5 to be suited for the use of INP prediction; lower correlation coefficients might still indicate significant relationships, however, are not suited for predicting the majority (>50% of the data) of INP concentrations observed. The INP concentrations are thereby compared individually to the tested parameter.

Table 1. Parameters and respective time resolution of meteorological variables, size distribution, and absorption measurements.

	Parameter	Time Resolution
Meteorology	RH_a (%)	60 min
	T_a (K)	10 min
	pressure (hPa)	
	wind velocity ($m\ s^{-1}$) wind direction ($^\circ$)	
Size-inferred	$N_{<0.1\ \mu m}$ (cm^{-3})	6 min
	$N_{0.1-0.5\ \mu m}$ (cm^{-3})	
	$N_{>0.5\ \mu m}$ (cm^{-3})	
	A_{tot} (m^{-3})	
Absorption	eBC ($ng\ m^{-3}$)	60 min
Chemistry	sulfate ($\mu g\ m^{-3}$)	24 h
	nitrate ($\mu g\ m^{-3}$)	
	chloride ($\mu g\ m^{-3}$)	
	gravimetric weight ($\mu g\ m^{-3}$)	

2.3. Identification of FT Conditions

The discrimination between FT and BLI is based on two criterions which have to be fulfilled simultaneously (see Lacher, et al. [58] for detailed description): The trace gas ratio of NO_y to CO is used to assess FT [60,61,77–79] because both species are emitted from anthropogenic sources; while CO is relatively constant on the time scale of few days to weeks, NO_y decreases with atmospheric age. As such, NO_y/CO gives information on the last boundary layer contact. The second criterion is the number concentration of accumulation mode aerosol particles >90 nm, which is an indication for BLI because this size of particles is not formed in the FT [60].

The influence of SDEs, which are transported within the FT, are identified with the single scattering albedo Angström exponent [62]. If the majority of the aerosol particles consist of Saharan dust,

the single scattering albedo Angström exponent decreases with increasing wavelength due to the specific chemical composition and size of this particle type.

Marine-influenced air masses in the FT are identified by the analysis of parallel sampled cloud water samples with regard to the fraction of strontium (Sr) coming from sea salt, based on the finding that the ratio of Sr to sodium (Na^+) is constant [80]; in addition, the ratio of the Na to Aluminum (Al) needs to be low in order to exclude mineral dust influence, which is naturally rich in Al. Details are given in Boose, et al. [30] and Lacher, et al. [69].

2.4. Comparison to Parameterization

DeMott et al. [15] performed INP and parallel aerosol measurements at quite distinct locations in the atmosphere: Airborne and ground-based measurements in North America, measurements over the Pacific basin, over a pristine rainforest site, and in the Arctic. They found that immersion freezing INP can be reasonably well predicted by $N_{>0.5 \mu\text{m}}$ at temperatures between 264 and 238 K, resulting in the following parameterization (D10):

$$\text{D10: } n_{\text{INP}}(T) = a \cdot (273.16 - T)^b \cdot (n_{p>0.5 \mu\text{m}})^{c \cdot (273.16 - T) + d}. \quad (1)$$

The parameterizations suggested by Fletcher [27] and Meyers, et al. [28] are not suited for comparison with the observed INPs in this study, since both were developed for temperatures warmer than 253 K, which is above the measurement temperature used in this study.

It was found that the representation of INPs in cloud and climate models need to be predictable by a factor of 10 in terms of concentrations, since higher deviations will impact the cloud microphysical and radiative properties in the models [81]. However, INP measurement methods also include uncertainties, and deviations between different sampling instruments occur by e.g., a factor of 3 [82]. For comparison to the D10 parameterization, we thus state a good (fair) agreement if more than 50% of the data fall within a factor of 2 (factor of 5).

3. Results and Discussions

INP concentrations presented in this study were sampled during 8 field campaigns in winter, spring, and summer between the years 2014–2017, with a total sampling time of 534 h, out of which 229 h refer to BLI, and 293 h to $\text{FT}_{\text{background}}$ (Table 2). Only during wintertime, the majority of the measurements were taken during $\text{FT}_{\text{background}}$ conditions, while spring and summer were dominated by BLI. This is in fair agreement with Herrmann, et al. [60], measuring FT conditions more than 60% in winter, and less than 20% and 30% in spring and summer, respectively. For a detailed description of the occurrence of SDEs and marine events, as well as on FT conditions of each individual campaign, see Lacher, et al. [58]. Values presented here may differ from Lacher et al. [58] since here we only consider measurements taken with HINC and as such exclude measurements from winter 2014 (presented in Boose, et al. [30]) which are included in Lacher et al. [58].

Table 2. Ice nucleating particle (INP) concentrations measured at the High Altitude Research Station Jungfrauoch (JFJ) with Horizontal Ice Nucleation Chamber (HINC) between 2014 and 2017; sampling times for all measurements are given in hours, along with respective percentages for the occurrence of boundary layer injections (BLI) and free troposphere ($\text{FT}_{\text{background}}$).

	Time (h)	BLI (%)	$\text{FT}_{\text{background}}$ (%)
all	534	43	55
spring (2015, 2016)	119	78	20
summer (2014, 2015, 2016)	155	65	36
winter (2015, 2016, 2017)	260	12	82

3.1. Distinction by Air Mass Type

3.1.1. Meteorological Conditions

INP concentrations given as the total of performed measurements (no seasonal or annual distinction) with a distinction for all, BLI and $FT_{\text{background}}$ conditions do not show a dependence on the meteorological parameters of T_a , pressure, and RH_a (Figure 1). This suggests that the INP population at the JFJ is not directly dependent on the weather situation and related processes, such as water uptake of the aerosols at elevated RH_a . Also, the weather-related aerosol transport to the JFJ does not consistently influence INP concentrations. We acknowledge that this finding might be different for other sampling locations, which are e.g., not surrounded by firn ice, and where direct emission of aerosols from the ground might have an impact. Furthermore, INP concentrations do not show a considerable difference between in- and out-of-cloud (Figure 2), which might be due to counteracting processes balancing each other. Wet-removal processes in clouds could lead to a decrease in INP concentrations, as observed by Stopelli, et al. [55] at a measurement temperature of 263. It is not expected that this process has a measurable influence on INP concentrations at 242 K, which is colder than the temperature at which ambient ice crystals form and get depleted in clouds at the sampling site. Although this process might take place, we cannot quantify it due to the exponential increase in INP concentration with decreasing temperature e.g., [27]. However, this effect might also be masked by excluding sampling of larger ice crystals ($>40 \mu\text{m}$) in the inlet systems at the JFJ, which would lead to a lower INP concentration in clouds. In addition, INP concentrations are independent of wind velocity, which indicates that our measurements were not influenced by blowing snow.

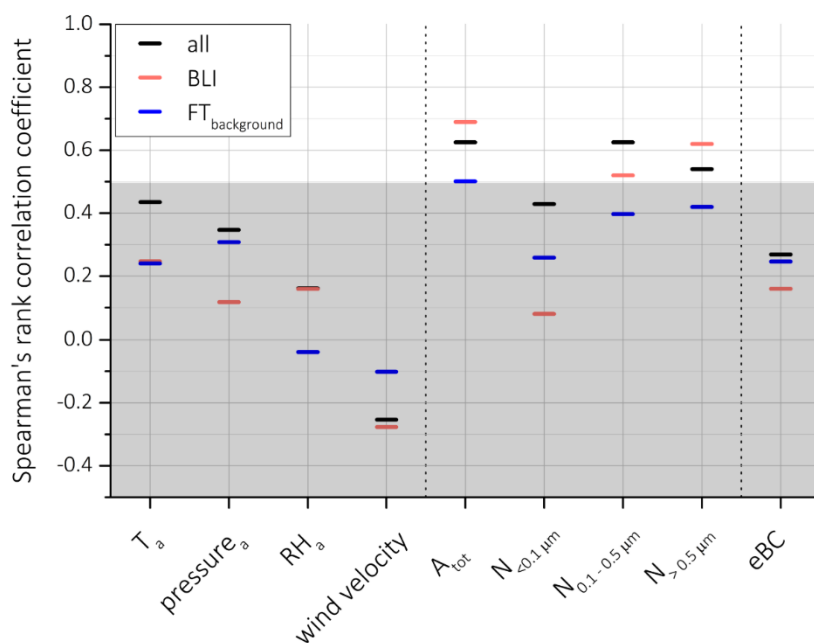


Figure 1. Spearman's rank correlation coefficient for ice nucleating particle (INP) concentrations (at $T = 242 \text{ K}$ and $RH_w = 104\%$) with meteorological and size inferred parameters and eBC for all conditions, BLI, and $FT_{\text{background}}$, for the total of the field campaigns. Low correlation coefficients (<0.5) are covered by grey shading. The 95% confidence intervals are within a maximum ± 0.003 of the respective Spearman's rank correlation coefficients, but are not visible on the presented scale.

In order to investigate possible source regions, INP concentrations sampled in air masses coming from the two main wind directions of north-west (NW) and south-east (SE) are shown in Figure 3. These two main wind directions are resulting from a channeling effect caused by the topography at the JFJ. Lugauer, et al. [52] found a reasonably well correlation with the measured wind directions at the JFJ and the wind direction at 500 hPa, as such the main wind directions are indeed representative for the

general wind flow. Significantly higher INP concentrations were measured in air masses from SE during all and BLI conditions. This is a first indication for a specific source of INPs. For a further investigation, we retrieved back trajectories with the Hybrid Single-Particle Lagrangian model (HYSPLIT; [83]) for air masses during BLI and coming exclusively from SE (Figure A1 in the Appendix A). They reveal that elevated INP concentrations ($>100 \text{ stdL}^{-1}$) were measured when the air masses passed over the heavily polluted region of the Po valley and industrial regions in France. As such, this might be an indication that anthropogenic activity can lead to temporal increases in INP concentrations at the JFJ. We acknowledge that some back trajectories which were started at the JFJ do not actually go into SE wind direction (see Figure A1), and is possibly related to the complex terrain of the site, which the HYSPLIT model is not able to resolve due to its low horizontal and vertical resolution.

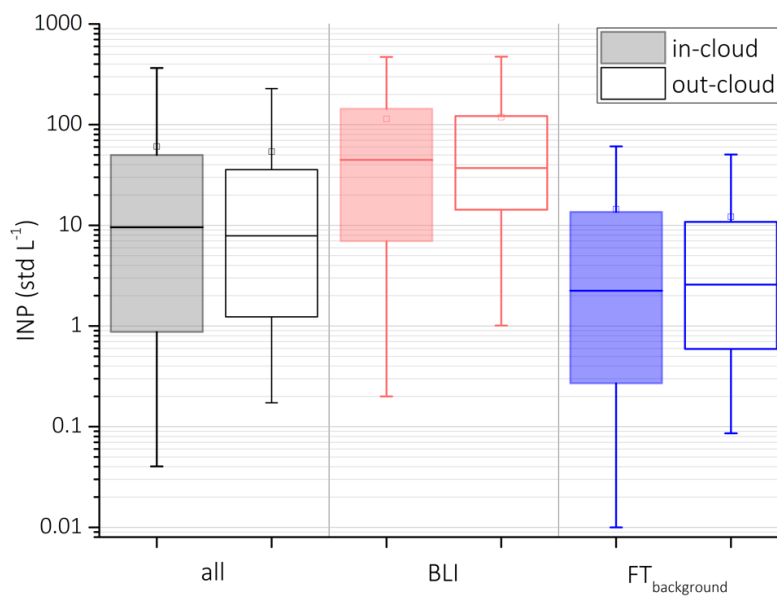


Figure 2. INP concentrations (242 K and $\text{RH}_w = 104\%$) distinguished into in- and out-of-cloud for all conditions, BLI, and $\text{FT}_{\text{background}}$.

Another interesting finding is that there is no significant difference in INP concentrations as a function of wind direction during $\text{FT}_{\text{background}}$ (Figure 3), which indicates that INP in the FT cannot be attributed to a specific source. This is not surprising given that air masses in such an environment are considered to be well mixed due to the longer time scales of mixing and transport into the FT [26], possibly leading to a homogeneous INP population.

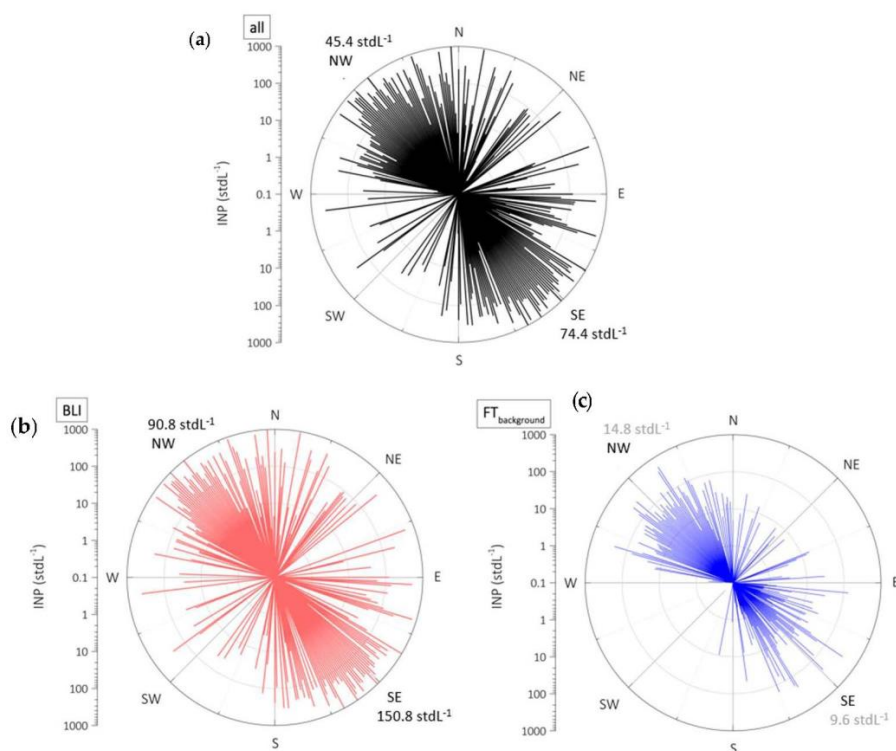


Figure 3. INP concentrations (242 K and $RH_w = 104\%$) as function of wind direction for (a) all conditions, (b) BLI, and (c) $FT_{background}$; median INP concentrations are given in the upper left (NW) and lower right (SE) corner; grey values refer to insignificant differences between INP concentrations from NW and SE.

3.1.2. Size Inferred Parameters and eBC

From the size-inferred parameters of the ambient aerosol particles, A_{tot} has the best relationship to INP concentrations during the discussed sampling conditions (Figure 1). This suggests the previously established concept of ice-active sites [84], which scales with the surface area of the aerosol particles. For all discussed conditions, correlation coefficients >0.5 are achieved, however, with higher values during BLI as compared to $FT_{background}$ conditions. An explanation for this difference might be that surface coating or modification of the aerosol particles, associated with atmospheric aging processes during long-range transport in the FT, could mask a relationship to A_{tot} by covering ice active sites. That such a process is indeed relevant in the FT is supported by a study of China, et al. [85], who found that a major fraction of particles sampled in the FT was coated with organic matter. We acknowledge that with the techniques used in this study, the effect of coating on ambient ice nucleation cannot be investigated directly, but can only be inferred indirectly.

Next to A_{tot} , aerosol particles in a specific size range might be suitable to predict INP concentrations as was done in DeMott, et al. [15]. Surprisingly, only for $N_{>0.1 \mu m}$ and for all and BLI conditions, a relationship to INP concentrations is revealed (Figure 1), suggesting that the ice active aerosol particles might be of sizes in the accumulation mode. The absence of a relationship to a specific size range in $FT_{background}$ points to the possibility that INPs in such conditions are multivariate, and not necessarily of one size or class. In addition, this finding supports the idea that INPs have a size threshold of >100 nm, which was first proposed by Pruppacher and Klett [6] and confirmed by more recent studies [8,9].

One specific aerosol class might be eBC . However, in this study, a strong correlation between INP concentrations and eBC was not found considering the total of performed measurements in any of the discussed conditions. This suggests that eBC does not have a major contribution to the INP population active at 242 K at the JFJ, which is in agreement to the findings of studies on the ice residuals of MPCs

at the same site [48,49]. This observation is also not surprising given previous laboratory studies of ice nucleation onto a variety of soot particles and sizes also concluded no heterogeneous freezing observed the mixed-phase temperature regime ($T > -38$ °C), and that cirrus temperatures were required to observe ice nucleation [50,51].

3.1.3. Chemical Compounds

The analysis of the PM10 filters reveals a significant correlation of INP concentrations with sulfate concentrations and the PM10 concentrations for all conditions (Figure 4). We believe that this is due to the influence from BLI, resulting in air masses which are enriched in sulfate and in total mass, and as well as in INP concentrations. However, due to the low time resolution of the filters, no distinction due to BLIs was possible. The correlation with the gravimetric weight suggests that the more material is present, the more likely it is to contain INPs, which was also indicated by the analysis of INP and A_{tot} . No significant correlation was found between INP concentrations and nitrate or sulfate, suggesting that INPs may not have been internally mixed with these species as has been found in other studies as well [86,87]. However, we note that we have very few data points to correlate INP with the PM species. Drawing a stronger conclusion on INP mixing state would require further studies. Also, the significant correlation for the sulfate concentrations and the gravimetric weight vanishes when the results are filtered for $FT_{background}$ conditions, again highlighting the complexity of ice nucleation in this environment. A negative significant correlation to chloride during all conditions was found, suggesting that air masses containing sea salt particles or chloride from other sources contain less ice nucleation active material. However, this is different from marine biogenic particulates which show significant ice nucleation activity when emitted or sampled from the ocean surface microlayer or from wave-breaking [14,40]. The ice nucleation activity of particles emitted from the ocean has been connected to biological activity of phytoplankton species [14,40,88], as such, it might be possible that marine particle sources still have an impact on ice nucleation, but not sea salt particles, as discussed in Kanji et al. [5] and references therein. We acknowledge that the time resolution of the presented comparison is very low and that high-time resolution measurements on chemical species or longer term monitoring of INP would be needed to clearly identify the contribution of these chemical species on ice nucleation.

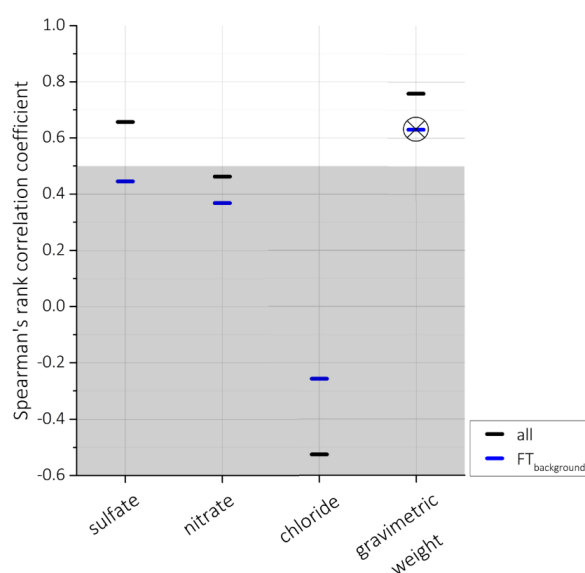


Figure 4. Spearman's rank correlation coefficient for INP concentrations with sulfate, nitrate, chlorite, and the gravimetrically determined PM10, for all and $FT_{background}$ conditions; PM10 filter measurements refer to 24 h sampling time, respective INP concentrations are referring to >9 h of this sampling time interval. Low correlation coefficients (<0.5) are covered by grey shading; crossed mark refers to insignificant correlation.

3.2. Distinction by Seasonal Variability and Air Mass Type

3.2.1. Meteorological Conditions

No relationship to meteorological conditions of T_a , pressure, and RH_a was determined for the sampling conditions discussed in the different seasons (Figure A2 in the Appendix A), as well as no difference between in- and out-cloud conditions (Figure A3 in the Appendix A). This strengthens our earlier conclusions that INP concentrations measured at 242 K in the immersion mode are independent of the weather situation.

Only the analysis of INP concentrations as a function of wind direction shows that during all conditions, air masses coming from the SE are significantly higher as compared to NW cases (Figure A4 in the Appendix A), but only during spring and summer (no significant difference in winter), when more BLIs prevail. This is also true for BLI, and also in the $FT_{background}$, when there are higher INP concentrations during spring from SE. The latter alludes to the contribution of anthropogenic influence from source regions which are mostly in SE directions. In addition, it might also be possible that the Saharan desert contributes to the background aerosol particle population given the frequency of SDEs at JFJ, but we believe that it is unlikely that Saharan dust coming from the BL contributes considerably to the INP population, since the dust particles are mostly transported to JFJ in the FT during long-range transport. Surprisingly, in winter the INP concentrations in the $FT_{background}$ are significantly higher when the sampled air masses are coming from NW, which might be an indication that the main source region of INPs in this season is different, as compared to others such as marine sources in the North Sea [69].

3.2.2. Size Inferred Parameters and eBC

The size-inferred parameters (except $N_{<0.1 \mu m}$) and eBC show some moderate correlations in the summer season during all conditions (Figure 5a), and during BLI (Figure 5b). While the wintertime measurements also correlate well with A_{tot} and $N_{<0.5 \mu m}$ during BLI, none of the investigated parameters shows a relationship with INP concentrations in spring, which might indicate that a parameter not investigated is controlling ice nucleation, as e.g., the influence from biological particles. In the $FT_{background}$, no relationship to the investigated parameter exists for any season (Figure 5c), which, again, might indicate that the dominating parameter is still unknown. However, another explanation might be that in such a remote, and well-mixed atmosphere, there is not a single particle type being the dominant INP source. Given that the FT is decoupled from the direct influence of BL, it is not surprising that there is no seasonal difference in the presented analysis for the FT.

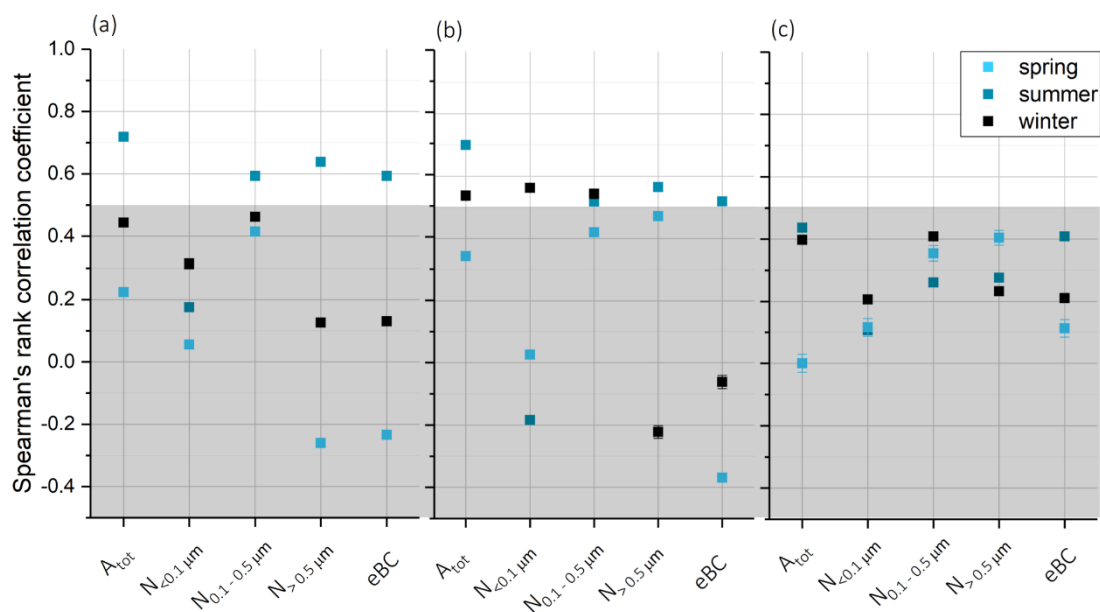


Figure 5. Spearman's rank correlation coefficient for INP concentrations with meteorological and size inferred parameters and eBC for all conditions, BLI, and $FT_{background}$ for the seasonal measurements; (a) refers to measurements under all conditions; (b) to BLI; (c) to $FT_{background}$. The 95% confidence intervals are within a maximum ± 0.03 of the respective Spearman's rank correlation coefficients as presented by the respective error bars.

3.3. Testing INP Parameterization

The D10 parameterization [15] is applied for BLI and $FT_{background}$ sampling conditions to test its applicability. Overall, the parameterization tends to underpredict elevated INP concentrations ($>10 \text{ stdL}^{-1}$) in the $FT_{background}$ (Figure 6). During $FT_{background}$ sampling conditions, only 53% of predicted INP concentrations are within a factor of 5 of measured values (Table 3). The discrepancies to D10 indicate that $N_{>0.5 \mu\text{m}}$ is not always dominating the INP population in the FT, and that smaller aerosol particles might be ice active. However, for BLI sampling conditions, there is a better agreement between predicted and observed INP concentrations, with 64% of the data falling within a factor of 5 (Figure 6 and Table 3). This is not surprising, given that the D10 parameterization was developed based on measurements taken mostly in the boundary layer.

A specific analysis only for $FT_{background}$ conditions yields that especially in the winter the underestimation of INP concentrations based on D10 is non-trivial (Figure 7). A minority of only 41% of the INP concentrations can be predicted by D10 within a factor 5 (52% in spring, and 58% in summer). This indicates that during this time the station might be regularly under the influence of an INP population with diameter $<0.5 \mu\text{m}$. Also in the study by Mason, et al. [32], it was found that at an alpine site and towards colder measurement temperatures (248 K), the size of the INPs did not exhibit a clear dependence on larger particles, and a considerable fraction of INPs were $<0.5 \mu\text{m}$.

We propose that the INP population in the $FT_{background}$ is not dominated by aerosol particles $>0.5 \mu\text{m}$ and that smaller particles need to be considered as INPs in such an environment.

Lastly, if considering a stringent comparison of within a factor of 2 for predicted vs. observed INPs, no good agreement is achieved in any discussed air mass condition. This is in some sense not surprising because ambient INPs often have a natural variability exceeding a factor of 2, thus any parameterization based on INP number concentration will have a challenge to constrain predicted INPs to within a factor of 2. In addition, instrument uncertainties add to this variability, as such we consider the evaluation of within a factor of 5 to be representative for the current state of ambient INP observations.

Table 3. Percentage of predicted INP concentrations that fall within a factor of 2 and 5 of the observed INP concentrations given for different sampling conditions, and non-seasonal (total) and seasonal distinction.

		Within Factor (%)	
		2	5
all	total	32	57
	spring	21	52
	summer	44	75
	winter	27	47
BLI	total	36	64
	spring	23	55
	summer	49	80
	winter	12	23
FT _{background}	total	30	53
	spring	20	52
	summer	33	58
	winter	20	41

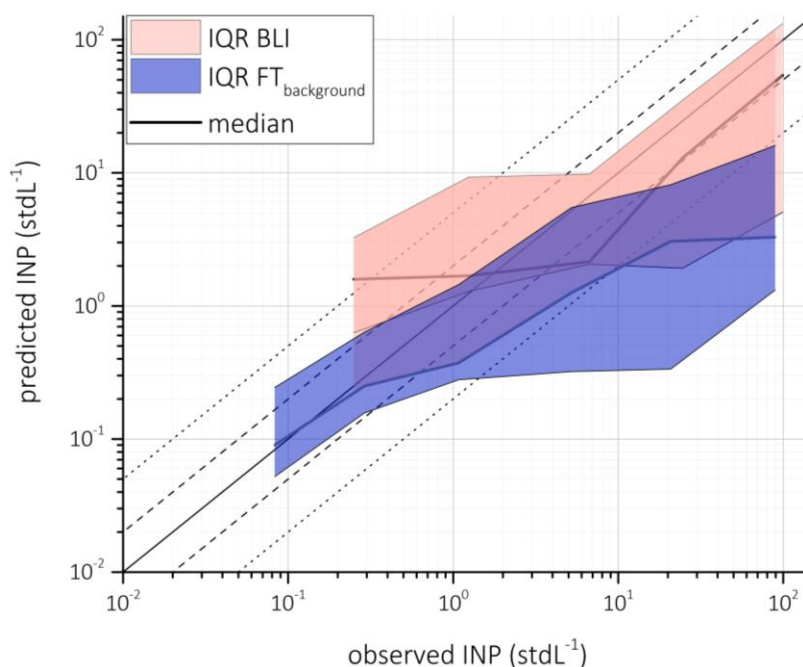


Figure 6. Predicted INP concentrations (D10) during FT_{background} (blue) and BLI (light red) at T = 242 K and RH_w = 104% as a function of observed INP concentrations; thick line give median INP concentrations, the filled area represents the inter-quartile range (25th to 75th quartile); the solid line represents the 1:1 fit, the long dashed lines represent a factor of 2, and the short dashed lines a factor of 5.

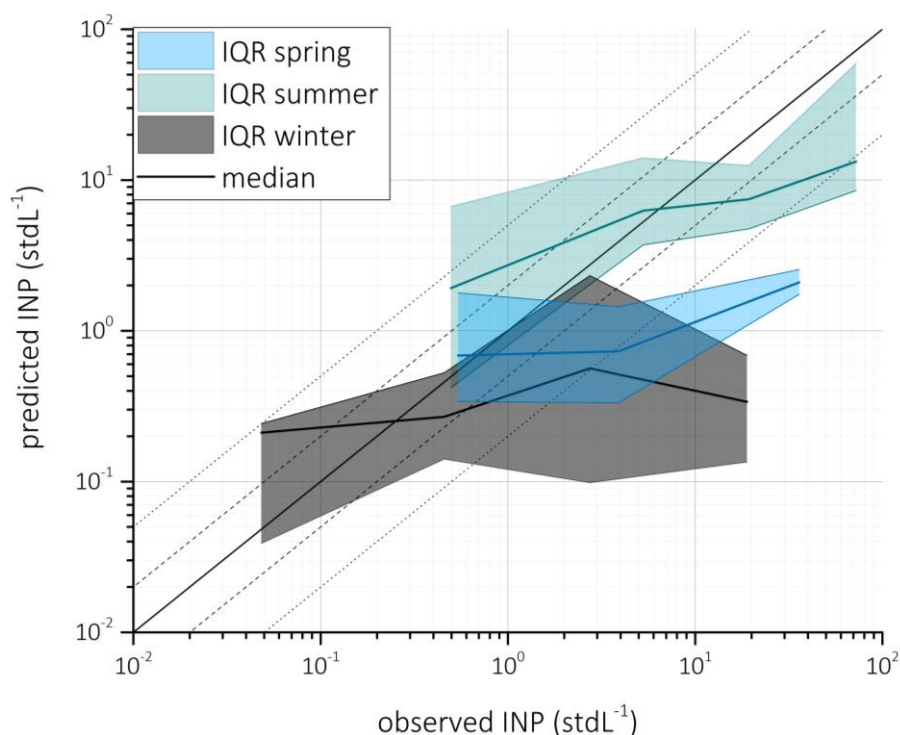


Figure 7. Predicted INP concentrations (D10) during $FT_{\text{background}}$ at $T = 242$ K and $RH_w = 104\%$ as a function of observed INP concentrations in the season of spring (blue), summer (green), and winter (grey); thick line give median INP concentrations, the filled area represents the inter-quartile range; the solid line represents the 1:1 fit, the long dashed lines represent a factor of 2, and the short dashed lines a factor of 5.

4. Conclusions

In this work, we investigate possible predictor parameters for INP concentrations as measured at 242 K and $RH_w = 104\%$ at the JFJ. Being located at 3580 m a.s.l. above a glacier, the site is usually exposed to FT air masses but can receive air mass injections from the local boundary layer. The data presented here were obtained during a total of eight field campaigns in spring, summer, and winter of the years 2014–2017. To date, these measurements represent the longest time series of online INP measurements at a field site and as such are suited to investigate parameters and processes influencing atmospherically relevant ice nucleation.

We find that most meteorological parameters are not related to INP concentrations at given measurement conditions, neither for the total performed measurements nor during the different seasons. This was found before during a single field campaign in winter by Boose, et al. [30] at the same site and at similar measurement conditions. Our results confirm this finding, revealing that this is also true for other seasons and years. Only the wind direction, an indicator for potential source regions, shows that air masses contained significantly higher INP concentrations during BLI from the SE. This might be an indication for the influence from anthropogenic activity, as e.g., from the Po valley in Northern Italy. However, more specific measurements with online chemical composition would be required to clearly identify the type of INP from such an influence. Detailed high-resolution chemistry of the aerosol particles was not available, as such this may shed some light on the nature of INPs at JFJ.

In general, the best parameter to prescribe INP concentrations is A_{tot} , which strengthens the concept of ice-active sites, scaling with the available surface area. However, this relationship is strongest during BLI, and less prominent during $FT_{\text{background}}$ conditions. This might be connected to ageing processes, resulting in particles coated with (in)organic material, thus inhibiting ice nucleation and rendering ice-active sites unavailable, a process which is relevant during the long-range transport in the

FT [87,89]. This is further strengthened in the seasonal analysis where the correlation of INP with A_{tot} during $FT_{background}$ vanishes, and furthermore none of the investigated size-related parameters show any relationship to INP concentration. We recommend the performance of more specific measurements to clearly identify the role of ageing on ice nucleation.

The data collected here were also used to test an empirical parameterization by DeMott, et al. [15]. We find that the parameterization is only able to predict 53% of measured INP concentrations within a factor of 5 during $FT_{background}$, and the parameterization tends to underpredict elevated INP concentrations. This might be caused by the assumption in the parameterizations that the particle concentration $>0.5 \mu\text{m}$ is dominating the relationship to INP concentration. It is possible, given that the abundance of larger particles is very low in the FT, that the INP population at the JFJ is dominated by particles $<0.5 \mu\text{m}$. More specific measurements are required to determine the size of INPs. This might help to improve our understanding of predominant INP sources, and furthermore help to accurately model INP transport processes. Interestingly, the parameterization performs better when considering BLI, and 64% of the INP concentrations can be predicted within a factor of 5.

Our findings highlight that the ice nucleation ability of aerosol in the FT are controlled by a complex combination of properties that are yet to be resolved. Also, we acknowledge that the presented correlation of parameters to the INP concentrations do not indicate causation, which is especially relevant given that INPs are a rare subset of the ambient particle population. To improve on this, detailed analysis on the single INPs would be needed to answer the question of their type, origin, and characteristics, which is beyond the scope of this work and not possible with the experimental set up used in the current work. More research is needed on the size and origin of INPs in the FT, in order to better predict which aerosol type(s) are INPs, or which environmental (if any) physical and chemical properties control the ice nucleation ability of aerosol particles.

Author Contributions: L.L. wrote the manuscript, with contributions from Z.A.K., L.L. conducted the INP measurements and analyzed the data. L.L. and Z.A.K. interpreted the INP data. A.Z. conducted part of the cloud water samples and analyzed and interpreted the data. N.B. and E.H. contributed data on size distributions and on absorption characteristics. M.S. contributed data on trace gases. Z.A.K. oversaw the overall project.

Funding: The research was funded by the Global Atmospheric Watch, Switzerland (MeteoSwiss GAW-CH+2014–2017). This project has also received financial support from the ACTRIS research infrastructure funded by the European Union (H2020-INFRAIA-2014-2015; grant agreement No. 654109) and the Swiss State Secretariat for Education, Research and Innovation (SERI) (contract number 15.0159-1).

Acknowledgments: The data presented in figures and tables are available under Doi: 10.3929/ethz-b-000290039. We thank the International Foundation High Altitude Research Station Jungfrauoch and Gornergrat (HFJG) for the support and the opportunity to perform measurements, with a special thanks to the custodians Maria and Urs Otz, Joan and Martin Fischer, Susanne and Felix Seiler. We thank MeteoSwiss for providing meteorological data. Trace gases measured at JFJ are part of the Swiss National Air Pollution Monitoring Network which is jointly run by EMPA and the Swiss Federal Office for the Environment. The opinions expressed and arguments employed herein do not necessarily reflect the official views of the Swiss Government. For fruitful discussions, we acknowledge Anina Gilgen and Ulrike Lohmann, and for technical support Hannes Wydler.

Conflicts of Interest: The authors declare no conflict of interest. The founding sponsors had no role in the design of the study; in the collection, analyses, or interpretation of data; in the writing of the manuscript, and in the decision to publish the results.

Appendix A

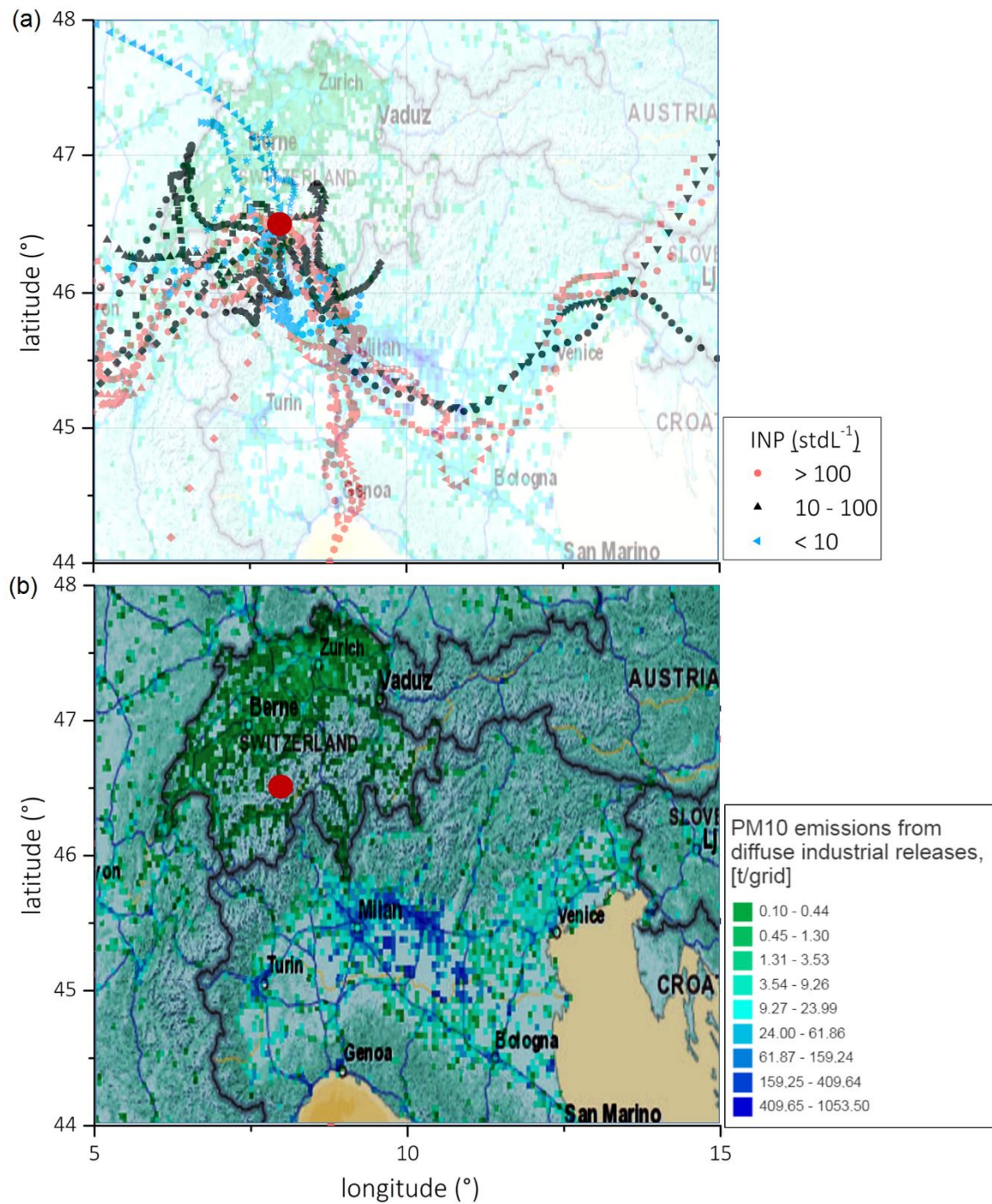


Figure A1. (a) HYSPLIT back trajectories [85] during BLI at the High Altitude Research Station Jungfrauoch (JFJ, red circle) for air masses from SE, with a time resolution of 1 h; back trajectories are categorized in INP concentrations; (b) particulate matter (PM10) emission from industrial sources [90] as indicator for anthropogenic emissions (available at <http://prtr.ec.europa.eu/#/diffemissionsair>).

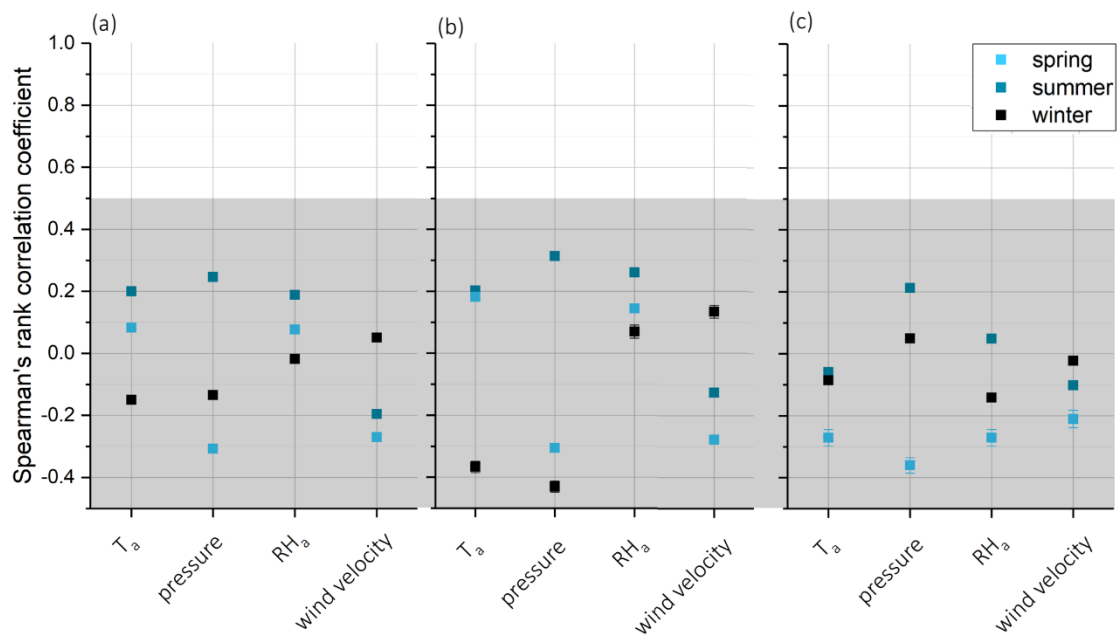


Figure A2. Spearman's rank correlation coefficient for INP concentrations with meteorological and size inferred parameters and eBC for all conditions, BLI, and $FT_{background}$ for the total and seasonal measurements; (a) refers to measurements under all conditions; (b) to BLI; (c) to $FT_{background}$. The 95% confidence intervals are within maximum ± 0.03 of the respective Spearman's rank correlation coefficients as presented by the respective error bars.

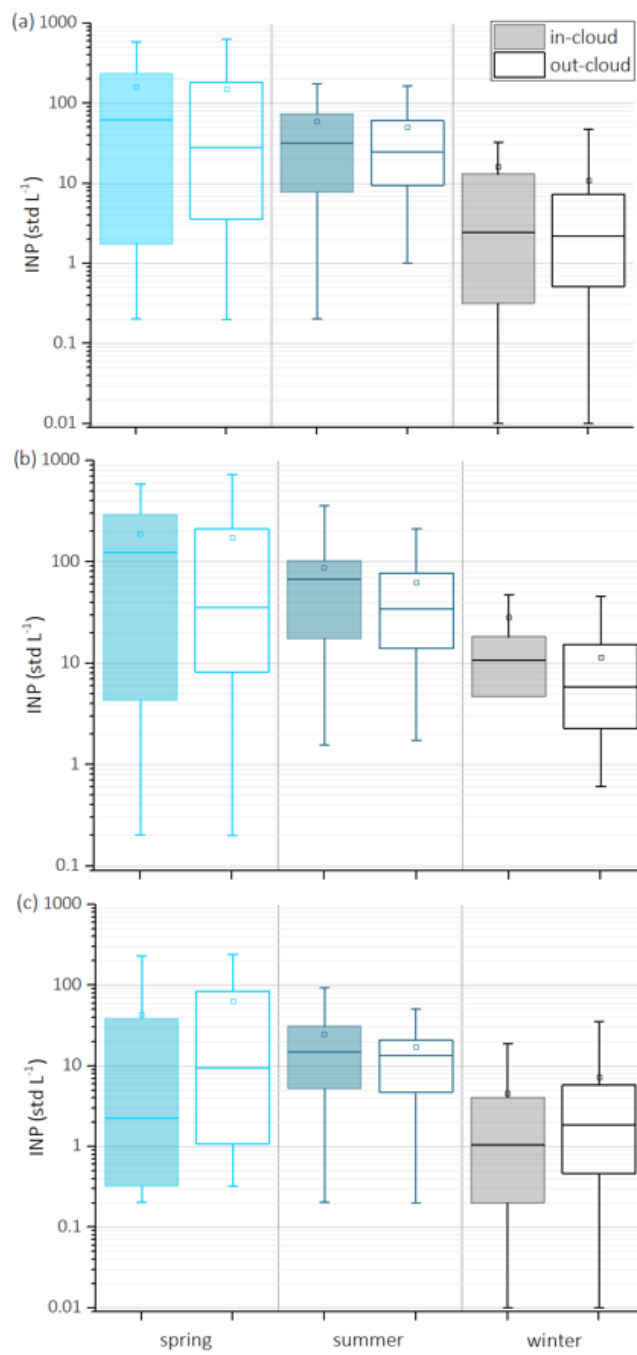


Figure A3. INP concentrations in- and out-of-cloud for all conditions (a), BLI (b), and $FT_{background}$ (c), distinguished into spring, summer, and winter measurements.

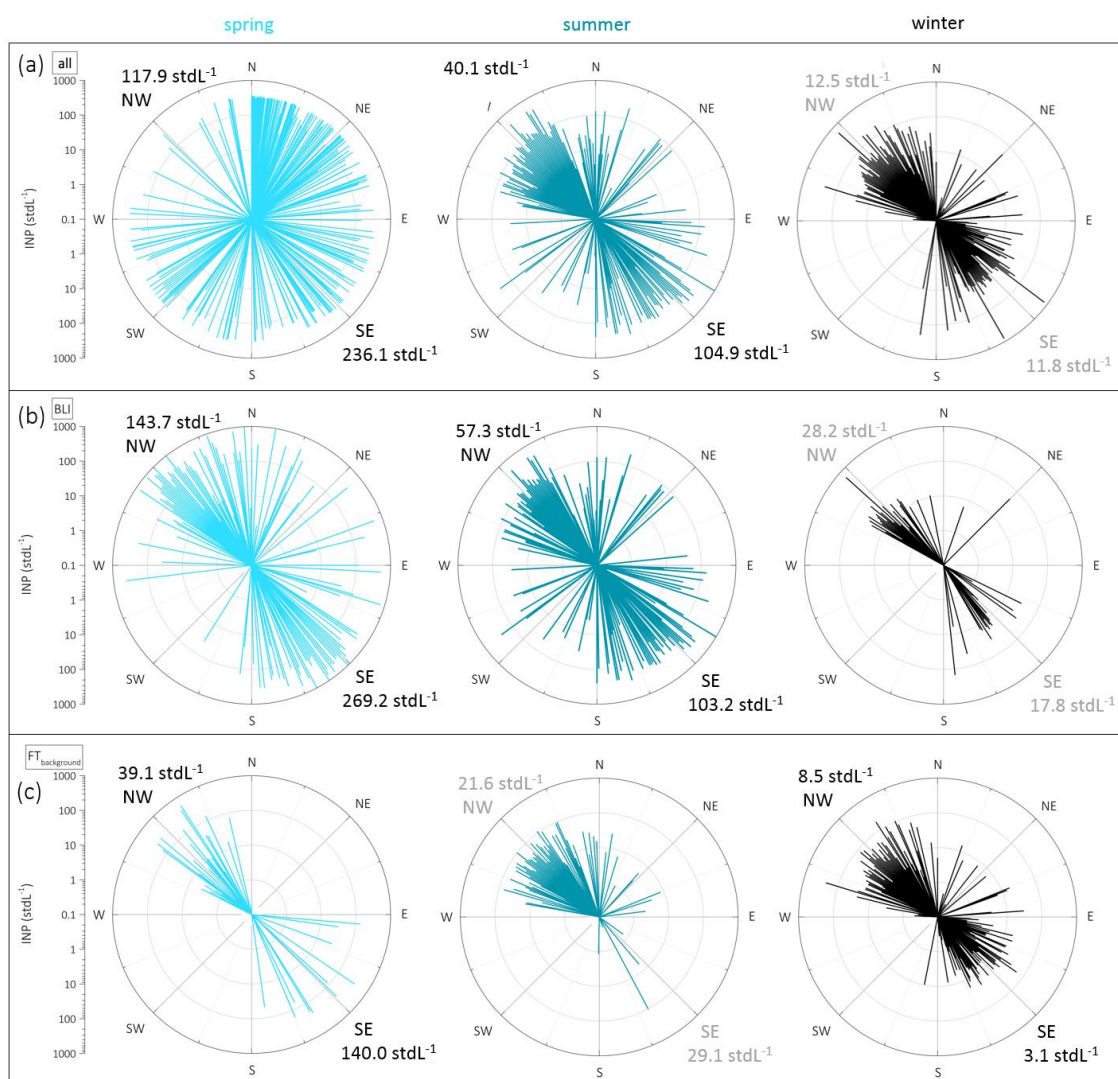


Figure A4. INP concentrations (242 K and $RH_w = 104\%$) as a function of wind direction during the seasons (light blue spring, blue summer, black winter) for (a) all conditions, (b) BLI, and (c) FT_{background}; median INP concentrations are given in the upper left (NW) and lower right (SE) corner; grey values refer to insignificant differences between INP concentrations from NW and SE.

References

1. Koop, T.; Luo, B.; Tsias, A.; Peter, T. Water activity as the determinant for homogeneous ice nucleation in aqueous solutions. *Nature* **2000**, *406*, 611–614. [[CrossRef](#)] [[PubMed](#)]
2. Vali, G.; DeMott, P.J.; Möhler, O.; Whale, T.F. Technical note: A proposal for ice nucleation terminology. *Atmos. Chem. Phys.* **2015**, *15*, 10263–10270. [[CrossRef](#)]
3. Korolev, A.; McFarquhar, G.; Field, P.R.; Franklin, C.; Lawson, P.; Wang, Z.; Williams, E.; Abel, S.J.; Axisa, D.; Borrmann, S.; et al. Mixed-phase clouds: Progress and challenges. *Meteorol. Monogr.* **2017**, *58*. [[CrossRef](#)]
4. Field, P.R.; Lawson, R.P.; Brown, P.R.A.; Lloyd, G.; Westbrook, C.; Moisseev, D.; Miltenberger, A.; Nenes, A.; Blyth, A.; Choulaton, T.; et al. Secondary ice production: Current state of the science and recommendations for the future. *Meteorol. Monogr.* **2017**, *58*. [[CrossRef](#)]
5. Kanji, Z.A.; Ladino, L.A.; Wex, H.; Boose, Y.; Burkert-Kohn, M.; Cziczo, D.J.; Krämer, M. Overview of ice nucleating particles. *Meteorol. Monogr.* **2017**, *58*. [[CrossRef](#)]
6. Pruppacher, H.R.; Klett, J.D. *Microphysics of Clouds and Precipitation*; Springer: Dordrecht, The Netherlands, 2010.
7. Archuleta, C.M.; DeMott, P.J.; Kreidenweis, S.M. Ice nucleation by surrogates for atmospheric mineral dust and mineral dust/sulfate particles at cirrus temperatures. *Atmos. Chem. Phys.* **2005**, *5*, 2617–2634. [[CrossRef](#)]

8. Kanji, Z.A.; Abbatt, J.P.D. Ice nucleation onto arizona test dust at cirrus temperatures: Effect of temperature and aerosol size on onset relative humidity. *J. Phys. Chem.* **2010**, *114*, 935–941. [[CrossRef](#)] [[PubMed](#)]
9. Welti, A.; Lüönd, F.; Stetzer, O.; Lohmann, U. Influence of particle size on the ice nucleating ability of mineral dusts. *Atmos. Chem. Phys.* **2009**, *9*, 6705–6715. [[CrossRef](#)]
10. Hoose, C.; Moehler, O. Heterogeneous ice nucleation on atmospheric aerosols: A review of results from laboratory experiments. *Atmos. Chem. Phys.* **2012**, *12*, 9817–9854. [[CrossRef](#)]
11. Després, V.; Huffman, J.; Burrows, S.; Hoose, C.; Safatov, A.; Buryak, G.; Fröhlich-Nowoisky, J.; Elbert, W.; Andreae, M.; Pöschl, U.; et al. Primary biological aerosol particles in the atmosphere: A review. *Tellus B Chem. Phys. Meteorol.* **2012**, *64*. [[CrossRef](#)]
12. Conen, F.; Stopelli, E.; Zimmermann, L. Clues that decaying leaves enrich arctic air with ice nucleating particles. *Atmos. Environ.* **2016**, *129*, 91–94. [[CrossRef](#)]
13. Creamean, J.M.; Suski, K.J.; Rosenfeld, D.; Cazorla, A.; DeMott, P.J.; Sullivan, R.C.; White, A.B.; Ralph, F.M.; Minnis, P.; Comstock, J.M.; et al. Dust and biological aerosols from the sahara and asia influence precipitation in the western U.S. *Science* **2013**, *339*, 1572–1578. [[CrossRef](#)] [[PubMed](#)]
14. DeMott, P.J.; Hill, T.C.J.; McCluskey, C.S.; Prather, K.A.; Collins, D.B.; Sullivan, R.C.; Ruppel, M.J.; Mason, R.H.; Irish, V.E.; Lee, T.; et al. Sea spray aerosol as a unique source of ice nucleating particles. *Proc. Natl. Acad. Sci. USA* **2016**, *113*, 5797–5803. [[CrossRef](#)] [[PubMed](#)]
15. DeMott, P.J.; Prenni, A.J.; Liu, X.; Kreidenweis, S.M.; Petters, M.D.; Twohy, C.H.; Richardson, M.S.; Eidhammer, T.; Rogers, D.C. Predicting global atmospheric ice nuclei distributions and their impacts on climate. *PNAS* **2010**, *107*, 11217–11222. [[CrossRef](#)] [[PubMed](#)]
16. Mason, R.H.; Si, M.; Li, J.; Chou, C.; Dickie, R.; Toom-Saunty, D.; Pöhlker, C.; Yakobi-Hancock, J.D.; Ladino, L.A.; Jones, K.; et al. Ice nucleating particles at a coastal marine boundary layer site: Correlations with aerosol type and meteorological conditions. *Atmos. Chem. Phys.* **2015**, *15*, 12547–12566. [[CrossRef](#)]
17. Prenni, A.J.; Tobo, Y.; Garcia, E.; DeMott, P.J.; Huffman, J.A.; McCluskey, C.S.; Kreidenweis, S.M.; Prenni, J.E.; Pöhlker, C.; Pöschl, U. The impact of rain on ice nuclei populations at a forested site in Colorado. *Geophys. Res. Lett.* **2013**, *40*, 227–231. [[CrossRef](#)]
18. Brooks, S.D.; Suter, K.; Olivarez, L. Effects of chemical aging on the ice nucleation activity of soot and polycyclic aromatic hydrocarbon aerosols. *J. Phys. Chem.* **2014**, *118*, 10036–10047. [[CrossRef](#)] [[PubMed](#)]
19. DeMott, P.J. An exploratory study of ice nucleation by soot aerosols. *J. Appl. Meteorol.* **1990**, *29*, 1072–1079. [[CrossRef](#)]
20. Gorbunov, B.; Baklanov, A.; Kakutkina, N.; Windsor, H.L.; Toumi, R. Ice nucleation on soot particles. *J. Aerosol Sci.* **2001**, *32*, 199–215. [[CrossRef](#)]
21. Grawe, S.; Augustin-Bauditz, S.; Hartmann, S.; Hellner, L.; Pettersson, J.B.C.; Prager, A.; Stratmann, F.; Wex, H. The immersion freezing behavior of ash particles from wood and brown coal burning. *Atmos. Chem. Phys.* **2016**, *16*, 13911–13928. [[CrossRef](#)]
22. Petters, M.D.; Parsons, M.T.; Prenni, A.J.; DeMott, P.J.; Kreidenweis, S.M.; Carrico, C.M.; Sullivan, A.P.; McMeeking, G.R.; Levin, E.; Wold, C.E.; et al. Ice nuclei emissions from biomass burning. *J. Geophys. Res. Atmos.* **2009**, *114*, D07209. [[CrossRef](#)]
23. Popovicheva, O.; Kireeva, E.; Persiantseva, N.; Khokhlova, T.; Shonija, N.; Tishkova, V.; Demirdjian, B. Effect of soot on immersion freezing of water and possible atmospheric implications. *Atmos. Res.* **2008**, *90*, 326–337. [[CrossRef](#)]
24. Umo, N.S.; Murray, B.J.; Baeza-Romero, M.T.; Jones, J.M.; Lea-Langton, A.R.; Malkin, T.L.; O'Sullivan, D.; Neve, L.; Plane, J.M.C.; Williams, A. Ice nucleation by combustion ash particles at conditions relevant to mixed-phase clouds. *Atmos. Chem. Phys.* **2015**, *15*, 5195–5210. [[CrossRef](#)]
25. Bond, T.C.; Doherty, S.J.; Fahey, D.W.; Forster, P.M.; Berntsen, T.; DeAngelo, B.J.; Flanner, M.G.; Ghan, S.; Kärcher, B.; Koch, D.; et al. Bounding the role of black carbon in the climate system: A scientific assessment. *J. Geophys. Res. Atmos.* **2013**, *118*, 5380–5552. [[CrossRef](#)]
26. Stull, R.B. *An Introduction to Boundary Layer Meteorology*; Springer: Dordrecht, The Netherlands, 1988.
27. Fletcher, N.H. *The Physics of Rainclouds*; Cambridge University Press: Cambridge, UK, 1962.
28. Meyers, M.P.; DeMott, P.J.; Cotton, W.R. New primary ice-nucleation parameterizations in an explicit cloud model. *J. Appl. Meteorol.* **1992**, *31*, 708–721. [[CrossRef](#)]
29. Ardon-Dryer, K.; Levin, Z.; Lawson, R.P. Characteristics of immersion freezing nuclei at the south pole station in antarctica. *Atmos. Chem. Phys.* **2011**, *11*, 4015–4024. [[CrossRef](#)]

30. Boose, Y.; Kanji, Z.A.; Kohn, M.; Sierau, B.; Zipori, A.; Crawford, I.; Lloyd, G.; Bukowiecki, N.; Herrmann, E.; Kupiszewski, P.; et al. Ice nucleating particle measurements at 241 K during winter months at 3580 m msl in the swiss alps. *J. Atmos. Sci.* **2016**, *73*, 2203–2228. [[CrossRef](#)]
31. Boose, Y.; Sierau, B.; García, M.I.; Rodríguez, S.; Alastuey, A.; Linke, C.; Schnaiter, M.; Kupiszewski, P.; Kanji, Z.A.; Lohmann, U. Ice nucleating particles in the saharan air layer. *Atmos. Chem. Phys.* **2016**, *16*, 9067–9087. [[CrossRef](#)]
32. Mason, R.H.; Si, M.; Chou, C.; Irish, V.E.; Dickie, R.; Elizondo, P.; Wong, R.; Brintnell, M.; Elsasser, M.; Lassar, W.M.; et al. Size-resolved measurements of ice-nucleating particles at six locations in north america and one in europe. *Atmos. Chem. Phys.* **2016**, *16*, 1637–1651. [[CrossRef](#)]
33. Prenni, A.J.; DeMott, P.J.; Sullivan, A.P.; Sullivan, R.C.; Kreidenweis, S.M.; Rogers, D.C. Biomass burning as a potential source for atmospheric ice nuclei: Western wildfires and prescribed burns. *Geophys. Res. Lett.* **2012**, *39*. [[CrossRef](#)]
34. Augustin, S.; Wex, H.; Niedermeier, D.; Pummer, B.; Grothe, H.; Hartmann, S.; Tomsche, L.; Clauss, T.; Voigtländer, J.; Ignatius, K.; et al. Immersion freezing of birch pollen washing water. *Atmos. Chem. Phys.* **2013**, *13*, 10989–11003. [[CrossRef](#)]
35. Fröhlich-Nowoisky, J.; Hill, T.C.J.; Pummer, B.G.; Yordanova, P.; Franc, G.D.; Pöschl, U. Ice nucleation activity in the widespread soil fungus *mortierella alpina*. *Biogeosciences* **2015**, *12*, 1057–1071. [[CrossRef](#)]
36. O'Sullivan, D.; Murray, B.J.; Ross, J.F.; Whale, T.F.; Price, H.C.; Atkinson, J.D.; Umo, N.S.; Webb, M.E. The relevance of nanoscale biological fragments for ice nucleation in clouds. *Sci. Rep.* **2015**, *5*, 8082. [[CrossRef](#)] [[PubMed](#)]
37. Pummer, B.G.; Bauer, H.; Bernardi, J.; Bleicher, S.; Grothe, H. Suspendable macromolecules are responsible for ice nucleation activity of birch and conifer pollen. *Atmos. Chem. Phys.* **2012**, *12*, 2541–2550. [[CrossRef](#)]
38. Rosinski, J.; Haagenson, P.L.; Nagamoto, C.T.; Parungo, F. Ice-forming nuclei of maritime origin. *J. Aerosol Sci.* **1986**, *17*, 23–46. [[CrossRef](#)]
39. Tong, H.J.; Ouyang, B.; Nikolovski, N.; Lienhard, D.M.; Pope, F.D.; Kalberer, M. A new electrodynamic balance (EDB) design for low-temperature studies: Application to immersion freezing of pollen extract bioaerosols. *Atmos. Meas. Tech.* **2015**, *8*, 1183–1195. [[CrossRef](#)]
40. Wilson, T.W.; Ladino, L.A.; Alpert, P.A.; Breckels, M.N.; Brooks, I.M.; Browse, J.; Burrows, S.M.; Carslaw, K.S.; Huffman, J.A.; Judd, C.; et al. A marine biogenic source of atmospheric ice-nucleating particles. *Nature* **2015**, *525*, 234–238. [[CrossRef](#)] [[PubMed](#)]
41. Hoose, C.; Kristjánsson, J.E.; Burrows, S.M. How important is biological ice nucleation in clouds on a global scale? *Environ. Res. Lett.* **2010**, *5*, 024009. [[CrossRef](#)]
42. Lohmann, U.; Diehl, K. Sensitivity studies of the importance of dust ice nuclei for the indirect aerosol effect on stratiform mixed-phase clouds. *J. Atmos. Sci.* **2006**, *63*, 968–982. [[CrossRef](#)]
43. Sesartic, A.; Lohmann, U.; Storelvmo, T. Modelling the impact of fungal spore ice nuclei on clouds and precipitation. *Environ. Res. Lett.* **2013**, *8*, 014029. [[CrossRef](#)]
44. Spracklen, D.V.; Heald, C.L. The contribution of fungal spores and bacteria to regional and global aerosol number and ice nucleation immersion freezing rates. *Atmos. Chem. Phys.* **2014**, *14*, 9051–9059. [[CrossRef](#)]
45. Ullrich, R.; Hoose, C.; Möhler, O.; Niemand, M.; Wagner, R.; Höhler, K.; Hiranuma, N.; Saathoff, H.; Leisner, T. A new ice nucleation active site parameterization for desert dust and soot. *J. Atmos. Sci.* **2017**, *74*, 699–717. [[CrossRef](#)]
46. Niemand, M.; Möhler, O.; Vogel, B.; Vogel, H.; Hoose, C.; Connolly, P.; Klein, H.; Bingemer, H.; DeMott, P.; Skrotzki, J.; et al. A particle-surface-area-based parameterization of immersion freezing on desert dust particles. *J. Atmos. Sci.* **2012**, *69*, 3077–3092. [[CrossRef](#)]
47. Phillips, V.T.J.; Demott, P.J.; Andronache, C.; Pratt, K.A.; Prather, K.A.; Subramanian, R.; Twohy, C. Improvements to an empirical parameterization of heterogeneous ice nucleation and its comparison with observations. *J. Atmos. Sci.* **2013**, *70*, 378–409. [[CrossRef](#)]
48. Kamphus, M.; Ettner-Mahl, M.; Klimach, T.; Drewnick, F.; Keller, L.; Cziczo, D.J.; Mertes, S.; Borrmann, S.; Curtius, J. Chemical composition of ambient aerosol, ice residues and cloud droplet residues in mixed-phase clouds: Single particle analysis during the cloud and aerosol characterization experiment (CLACE 6). *Atmos. Chem. Phys.* **2010**, *10*, 8077–8095. [[CrossRef](#)]

49. Kupiszewski, P.; Zanatta, M.; Mertes, S.; Vochezer, P.; Lloyd, G.; Schneider, J.; Schenk, L.; Schnaiter, M.; Baltensperger, U.; Weingartner, E.; et al. Ice residual properties in mixed-phase clouds at the high-alpine Jungfrauoch site. *J. Geophys. Res. Atmos.* **2016**, *121*, 12343–312362. [[CrossRef](#)] [[PubMed](#)]
50. Mahrt, F.; Marcolli, C.; David, R.O.; Grönquist, P.; Barthazy Meier, E.J.; Lohmann, U.; Kanji, Z.A. Ice nucleation abilities of soot particles determined with the horizontal ice nucleation chamber. *Atmos. Chem. Phys. Discuss.* **2018**, *2018*, 1–41. [[CrossRef](#)]
51. Koehler, K.A.; DeMott, P.J.; Kreidenweis, S.M.; Popovicheva, O.B.; Petters, M.D.; Carrico, C.M.; Kireeva, E.D.; Khokhlova, T.D.; Shonija, N.K. Cloud condensation nuclei and ice nucleation activity of hydrophobic and hydrophilic soot particles. *Phys. Chem. Chem. Phys.* **2009**, *11*, 7906–7920. [[CrossRef](#)] [[PubMed](#)]
52. Lugauer, M.; Baltensperger, U.; Furger, M.; Gäggeler, H.W.; Jost, D.T.; Schwikowski, M.; Wanner, H. Aerosol transport to the high alpine sites jungfrauoch (3454 m a.s.l.) and colle gnifetti (4452 m a.s.l.). *Tellus B Chem. Phys. Meteorol.* **1998**, *50*, 76–92. [[CrossRef](#)]
53. Coen, C.M.; Weingartner, E.; Furger, M.; Nyeki, S.; Prévôt, A.S.H.; Steinbacher, M.; Baltensperger, U. Aerosol climatology and planetary boundary influence at the Jungfrauoch analyzed by synoptic weather types. *Atmos. Chem. Phys.* **2011**, *11*, 5931–5944. [[CrossRef](#)]
54. Harrison, A.D.; Whale, T.F.; Carpenter, M.A.; Holden, M.A.; Neve, L.; O'Sullivan, D.; Vergara Temprado, J.; Murray, B.J. Not all feldspars are equal: A survey of ice nucleating properties across the feldspar group of minerals. *Atmos. Chem. Phys.* **2016**, *16*, 10927–10940. [[CrossRef](#)]
55. Stopelli, E.; Conen, F.; Morris, C.E.; Herrmann, E.; Bukowiecki, N.; Alewell, C. Ice nucleation active particles are efficiently removed by precipitating clouds. *Sci. Rep.* **2015**, *5*, 16433. [[CrossRef](#)] [[PubMed](#)]
56. Beck, A.; Henneberger, J.; Fugal, J.P.; David, R.O.; Lacher, L.; Lohmann, U. Impact of surface and near-surface processes on ice crystal concentrations measured at mountain-top research stations. *Atmos. Chem. Phys. Discuss.* **2017**, *18*, 8909–8927. [[CrossRef](#)]
57. Conen, F.; Rodríguez, S.; Hüglin, C.; Henne, S.; Herrmann, E.; Bukowiecki, N.; Alewell, C. Atmospheric ice nuclei at the high-altitude observatory Jungfrauoch, Switzerland. *Tellus B Chem. Phys. Meteorol.* **2015**, *67*. [[CrossRef](#)]
58. Lacher, L.; DeMott, P.J.; Levin, E.J.T.; Suski, K.J.; Boose, Y.; Zipori, A.; Herrmann, E.; Bukowiecki, N.; Steinbacher, M.; Gute, E.; et al. Background free-tropospheric ice nucleating particle concentrations at mixed-phase cloud conditions. *J. Geophys. Res. Atmos.* **2018**, *123*. [[CrossRef](#)]
59. Griffiths, A.D.; Parkes, S.D.; Chambers, S.D.; McCabe, M.F.; Williams, A.G. Improved mixing height monitoring through a combination of lidar and radon measurements. *Atmos. Meas. Tech.* **2013**, *6*, 207–218. [[CrossRef](#)]
60. Herrmann, E.; Weingartner, E.; Henne, S.; Vuilleumier, L.; Bukowiecki, N.; Steinbacher, M.; Conen, F.; Collaud Coen, M.; Hammer, E.; Jurányi, Z.; et al. Analysis of long-term aerosol size distribution data from jungfrauoch with emphasis on free tropospheric conditions, cloud influence, and air mass transport. *J. Geophys. Res. Atmos.* **2015**, *120*, 9459–9480. [[CrossRef](#)]
61. Zellweger, C.; Forrer, J.; Hofer, P.; Nyeki, S.; Schwarzenbach, B.; Weingartner, E.; Ammann, M.; Baltensperger, U. Partitioning of reactive nitrogen (NO_x) and dependence on meteorological conditions in the lower free troposphere. *Atmos. Chem. Phys.* **2003**, *3*, 779–796. [[CrossRef](#)]
62. Collaud Coen, M.; Weingartner, E.; Schaub, D.; Hueglin, C.; Corrigan, C.; Henning, S.; Schwikowski, M.; Baltensperger, U. Saharan dust events at the jungfrauoch: Detection by wavelength dependence of the single scattering albedo and first climatology analysis. *Atmos. Chem. Phys.* **2004**, *4*, 2465–2480. [[CrossRef](#)]
63. Cui, J.; Pandey Deolal, S.; Sprenger, M.; Henne, S.; Staehelin, J.; Steinbacher, M.; Nédélec, P. Free tropospheric ozone changes over europe as observed at jungfrauoch (1990–2008): An analysis based on backward trajectories. *J. Geophys. Res. Atmos.* **2011**, *116*, D10304. [[CrossRef](#)]
64. Chou, C.; Stetzer, O.; Weingartner, E.; Juranyi, Z.; Kanji, Z.A.; Lohmann, U. Ice nuclei properties within a sahara dust event at the jungfrauoch in the swiss alps. *Atmos. Chem. Phys.* **2011**, *11*, 4725–4738. [[CrossRef](#)]
65. Baltensperger, U.; Gäggeler, H.W.; Jost, D.T.; Lugauer, M.; Schwikowski, M.; Weingartner, E. Aerosol climatology at the high-alpine site Jungfrauoch, Switzerland. *J. Geophys. Res.* **1997**, *102*, 19707–19715. [[CrossRef](#)]
66. Bukowiecki, N.; Weingartner, E.; Gysel, M.; Collaud Coen, M.; Zieger, P.; Herrmann, E.; Steinbacher, M.; Gäggeler, H.W.; Baltensperger, U. A review of more than 20 years of aerosol observation at the high altitude research station Jungfrauoch, Switzerland (3580 m a.s.l.). *Aerosol Air Qual. Res.* **2016**, *16*, 764–788. [[CrossRef](#)]

67. Steinbacher, M.; Wyss, S.; Emmenegger, L.; Hüglin, C. National Air Pollution Monitoring Network (NABEL). Available online: <https://www.hfsjg.ch/en/publications/activity-reports/> (accessed on 1 January 2018).
68. Appenzeller, C.; Begert, M.; Zenklusen, E.; Scherrer, S.C. Monitoring climate at jungfrauoch in the high swiss alpine region. *Sci Total Environ.* **2008**, *391*, 262–268. [[CrossRef](#)] [[PubMed](#)]
69. Lacher, L.; Lohmann, U.; Boose, Y.; Zipori, A.; Herrmann, E.; Bukowiecki, N.; Steinbacher, M.; Kanji, Z.A. The horizontal ice nucleation chamber (HINC): Inp measurements at conditions relevant for mixed-phase clouds at the high altitude research station Jungfrauoch. *Atmos. Chem. Phys.* **2017**, *17*, 15199–15224. [[CrossRef](#)]
70. Weingartner, E.; Nyeki, S.; Baltensperger, U. Seasonal and diurnal variation of aerosol size distributions ($10 < d < 750$ nm) at a high-alpine site (Jungfrauoch 3580 m a.s.l.). *J. Geophys. Res.* **1999**, *104*, 26809–26820.
71. Sjogren, S.; Gysel, M.; Weingartner, E.; Alfarra, M.R.; Duplissy, J.; Cozic, J.; Crosier, J.; Coe, H.; Baltensperger, U. Hygroscopicity of the submicrometer aerosol at the high-alpine site Jungfrauoch, 3580 m a.s.l., Switzerland. *Atmos. Chem. Phys.* **2008**, *8*, 5715–5729. [[CrossRef](#)]
72. VDI-Richtlinie: VDI 2463 Blatt 11 Messen von Partikeln—Messen der Massenkonzentration (Immission)—Filterverfahren—Filterwechsel Digital DA-80H. Available online: <https://www.din.de/en/wdc-beuth:din21:1182655/toc-7266891/download> (accessed on 1 October 1996).
73. Bruggisser, N.; Bruggisser, T.; Buchmann, B.; Bugmann, S.; Fischer, A.; Gehrig, R.; Graf, P.; Hill, M.; Hueglin, C.; Nyffeler, U.; et al. *Technischer Bericht zum Nationalen Beobachtungsnetz für Luftfremdstoffe (NABEL); EMPA: Dübendorf, Switzerland, 2016.* (In German)
74. Zellweger, C.; Steinbacher, M.; Buchmann, B. Evaluation of new laser spectrometer techniques for in-situ carbon monoxide measurements. *Atmos. Meas. Tech.* **2012**, *5*, 2555–2567. [[CrossRef](#)]
75. Zipori, A.; Rosenfeld, D.; Shpund, J.; Steinberg, D.M.; Erel, Y. Targeting and impacts of Agi cloud seeding based on rain chemical composition and cloud top phase characterization. *Atmos. Res.* **2012**, *114*, 119–130. [[CrossRef](#)]
76. Zipori, A.; Rosenfeld, D.; Tirosh, O.; Teutsch, N.; Erel, Y. Effects of aerosol sources and chemical compositions on cloud drop sizes and glaciation temperatures. *J. Geophys. Res. Atmos.* **2015**, *120*, 9653–9669. [[CrossRef](#)]
77. Griffiths, A.D.; Conen, F.; Weingartner, E.; Zimmermann, L.; Chambers, S.D.; Williams, A.G.; Steinbacher, M. Surface-to-mountaintop transport characterised by radon observations at the Jungfrauoch. *Atmos. Chem. Phys.* **2014**, *14*, 12763–12779. [[CrossRef](#)]
78. Pandey Deolal, S.; Staehelin, J.; Brunner, D.; Cui, J.; Steinbacher, M.; Zellweger, C.; Henne, S.; Vollmer, M.K. Transport of pan and noy from different source regions to the swiss high alpine site Jungfrauoch. *Atmos. Environ.* **2013**, *64*, 103–115. [[CrossRef](#)]
79. Zanis, P.; Ganser, A.; Zellweger, C.; Henne, S.; Steinbacher, M.; Staehelin, J. Seasonal variability of measured ozone production efficiencies in the lower free troposphere of central europe. *Atmos. Chem. Phys.* **2007**, *7*, 223–236. [[CrossRef](#)]
80. Turekian, K.K. *Oceans*; Prentice-Hall: Upper Saddle River, NJ, USA, 1968.
81. Phillips, V.T.J.; Choulaton, T.W.; Illingworth, A.J.; Hogan, R.J.; Field, P.R. Simulations of the glaciation of a frontal mixed-phase cloud with the explicit microphysics model. *Q. J. R. Meteorol. Soc.* **2003**, *129*, 1351–1371. [[CrossRef](#)]
82. Burkert-Kohn, M.; Wex, H.; Welti, A.; Hartmann, S.; Grawe, S.; Hellner, L.; Herenz, P.; Atkinson, J.D.; Stratmann, F.; Kanji, Z.A. Leipzig ice nucleation chamber comparison (LINC): Intercomparison of four online ice nucleation counters. *Atmos. Chem. Phys.* **2017**, *17*, 11683–11705. [[CrossRef](#)]
83. Stein, A.F.; Draxler, R.R.; Rolph, G.D.; Stunder, B.J.B.; Cohen, M.D.; Ngan, F. Noaa’s hysplit atmospheric transport and dispersion modeling system. *Bull. Am. Meteorol. Soc.* **2015**, *96*, 2059–2077. [[CrossRef](#)]
84. Vali, G. Quantitative evaluation of experimental results an the heterogeneous freezing nucleation of supercooled liquids. *J. Atmos. Sci.* **1971**, *28*, 402–409. [[CrossRef](#)]
85. China, S.; Alpert, P.A.; Zhang, B.; Schum, S.; Dzepina, K.; Wright, K.; Owen, R.C.; Fialho, P.; Mazzoleni, L.R.; Mazzoleni, C.; et al. Ice cloud formation potential by free tropospheric particles from long-range transport over the northern atlantic ocean. *J. Geophys. Res. Atmos* **2017**, *122*, 3065–3079. [[CrossRef](#)]
86. Cziczo, D.J.; Froyd, K.D.; Hoose, C.; Jensen, E.J.; Diao, M.; Zondlo, M.A.; Smith, J.B.; Twohy, C.H.; Murphy, D.M. Clarifying the dominant sources and mechanisms of cirrus cloud formation. *Science* **2013**, *340*, 1320–1324. [[CrossRef](#)] [[PubMed](#)]

87. DeMott, P.J.; Cziczo, D.J.; Prenni, A.J.; Murphy, D.M.; Kreidenweis, S.M.; Thomson, D.S.; Borys, R.; Rogers, D.C. Measurements of the concentration and composition of nuclei for cirrus formation. *Proc. Natl. Acad. Sci. USA* **2003**, *100*, 14655–14660. [[CrossRef](#)] [[PubMed](#)]
88. McCluskey, C.S.; Hill, T.C.J.; Sultana, C.M.; Laskina, O.; Trueblood, J.; Santander, M.V.; Beall, C.M.; Michaud, J.M.; Kreidenweis, S.M.; Prather, K.A.; et al. A mesocosm double feature: Insights into the chemical makeup of marine ice nucleating particles. *J. Atmos. Sci.* **2018**, *75*, 2405–2423. [[CrossRef](#)]
89. Richardson, M.S.; DeMott, P.J.; Kreidenweis, S.M.; Cziczo, D.J.; Dunlea, E.J.; Jimenez, J.L.; Thomson, D.S.; Ashbaugh, L.L.; Borys, R.D.; Westphal, D.L.; et al. Measurements of heterogeneous ice nuclei in the western United States in springtime and their relation to aerosol characteristics. *J. Geophys. Res. Atmos* **2007**, *112*. [[CrossRef](#)]
90. Theloke, J.; Thiruchittampalam, B.; Orlikova, S.; Uzbasich, M.; Gauger, T. Methodology Development for the Spatial Distribution of the Diffuse Emissions in Europe. Available online: <http://prtr.ec.europa.eu/#/diffemissionsair> (accessed on 9 May 2018).



© 2018 by the authors. Licensee MDPI, Basel, Switzerland. This article is an open access article distributed under the terms and conditions of the Creative Commons Attribution (CC BY) license (<http://creativecommons.org/licenses/by/4.0/>).